THE JOURNAL OF BIOLOGICAL CHEMISTRY VOL. 285, NO. 36, pp. 27944–27957, September 3, 2010

Synthetic Triterpenoids Target the Arp2/3 Complex and Inhibit Branched Actin Polymerization*[S]

Received for publication, January 12, 2010, and in revised form, June 16, 2010 Published, JBC Papers in Press, June 21, 2010, DOI 10.1074/jbc.M110.103036

Ciric To[‡], Brian H. Shilton[§], and Gianni M. Di Guglielmo[‡1]

From the Departments of [‡]Physiology and Pharmacology and [§]Biochemistry, Medical Sciences Building, University of Western Ontario, London, Ontario N6A 5C1, Canada

Synthetic triterpenoids are anti-tumor agents that affect numerous cellular functions including apoptosis and growth inhibition. Here, we used mass spectrometric and protein array approaches and uncovered that triterpenoids associate with proteins of the actin cytoskeleton, including actin-related protein 3 (Arp3). Arp3, a subunit of the Arp2/3 complex, is involved in branched actin polymerization and the formation of lamellipodia. 2-cyano-3,12-dioxooleana-1,9-dien-28-oic acid (CDDO)-Im and CDDO-Me were observed to 1) inhibit the localization of Arp3 and actin at the leading edge of cells, 2) abrogate cell polarity, and 3) inhibit Arp2/3-dependent branched actin polymerization. We confirmed our drug effects with siRNA targeting of Arp3 and observed a decrease in Rat2 cell migration. Taken together, our data suggest that synthetic triterpenoids target Arp3 and branched actin polymerization to inhibit cell migration.

Cell migration is crucial in many physiological processes such as embryogenesis, cell differentiation, cell renewal, and immune system responses. During these processes, cells undergo highly regulated and coordinated cell migration to enable growth or repair of cells. Cell migration is also important in the metastasis of tumor cells. Indeed, it is a hallmark of the most aggressive and advanced epithelial tumors prior to entering the metastatic stage. These tumor cells often undergo epithelial to mesenchymal transition and migrate in a deregulated manner. As a result, they invade other tissues and take over the host organism (1), causing 90% of cancer-related deaths (2).

Cell migration occurs through the coordination of numerous cellular proteins. This process includes directional sensing of cells, anchorage of cells at the leading edge, and the reorganization of different components in the cell to assist in cell movement. The orientation of cell movement is largely dependent on the reorganization of the cytoskeleton, which consists of microtubules, intermediate filaments, and actin cytoskeleton. Although microtubules, intermediate filaments, and leading edge proteins are pivotal in the structure and organization of migrating cells, the actin cytoskeleton also plays an essential role in cell polarity and cell migration. For instance, actin is involved in the formation of the lamellipodia and filopodia, which are membrane and finger-like projections, respectively, at the leading edge of migrating cells. Both lamellipodia and filopodia are important for directional and environmental sensing even though they may be formed through two distinct actin-assembly machineries with different actin dynamic properties (3). Lamellipodia are formed by actin-related protein 2/3 (Arp2/3)[2] complexes through branched actin nucleation, whereas filopodia are formed by formin by progressive unbranched actin nucleation. Although the processes of the two are similar in that they are both activated by small Rho GTPases and a nucleation-promoting factor is required for actin polymerization, the key effectors that enable these processes are distinct. For instance, Cdc42 activates neural Wiskott-Aldrich Syndrome protein (n-WASp), which in turn promotes nucleation and branched actin polymerization, whereas the activation of the RhoA induces formin-dependent unbranched actin polymerization. Interestingly, Rac1, another small Rho GTPase, has been shown to be involved both indirectly and directly in branched and unbranched actin polymerization, respectively. The understanding of the two distinct actin polymerization processes is crucial in understanding how cell migration is coordinated with other key cellular processes.

Because cell migration is a precursor event of cancer metastasis, chemotherapeutic agents that block cell migration have been an important focus in the field of cancer chemotherapy. Recently, the parental synthetic oleanane triterpenoid (CDDO) and its more potent derivatives (CDDO-Im and CDDO-Me) have been suggested to be promising therapeutic agents. Specifically, CDDO and its methyl ester (CDDO-Me) and imidazolide (CDDO-Im) derivatives have been shown to inhibit tumor growth and induce apoptosis (4–18). CDDO and its derivatives also disrupt the intracellular reduction-oxidation reaction balance (19–24) and are potent suppressors of nitric oxide production and at least two inflammatory enzymes, iNOS and COX-2, which are implicated with enhanced carcinogenesis in many organs (25). These mechanisms have been evident in various cancers including lymphoma (26–30), leukemia (12, 26, 31–35), glioblastoma (36), neuroblastoma (36), osteosarcoma (37), and cancer cell lines of the lung (8, 38–41), breast (10, 42–44), ovaries (45), pancreas (46), colon (5), and prostate (6). In addition, CDDO-based compounds have been shown to

* This work was supported by National Cancer Institute of Canada Grant 17189 and Canadian Institutes of Health Research Grant MOP-93625.

[S] The on-line version of this article (available at http://www.jbc.org) contains supplemental Fig. S1 and Movie S1.

[1] To whom correspondence should be addressed. Tel.: 519-661-2111 (ext. 80042); E-mail: john.diguglielmo@schulich.uwo.ca.

[2] The abbreviations used are: Arp, actin-related protein; n-WASp, neural Wiskott-Aldrich Syndrome protein; TRAIL, tumor necrosis factor-related apoptosis-inducing ligand; CDDO, 2-cyano-3,12-dioxooleana-1,9-dien-28-oic acid; b-CDDO, biotinylated CDDO; b-CDDO-Me, biotinylated CDDO-Me; CDDO-Im, CDDO-imidazolide; DMSO, dimethyl sulfoxide; DIC, differential interference contrast.

sensitize resistant CLL B cells (47) and TRAIL (tumor necrosis factor-related apoptosis-inducing ligand)-resistant cancer cells to induce apoptosis (43, 48). However, even though recent studies have shown that CDDO-Im is highly effective in various cancer cell lines and animal studies for inhibiting tumor growth and inducing apoptosis, the effect of the synthetic triterpenoids on cell migration and metastasis remains unclear. Thus far, CDDO-Im has been shown to target proteins at the leading edge of the cells and cause the disruption of the microtubule network through a mechanism that differs from microtubule-depolymerizing agents such as nocodazole (49). The present study aims to explore in further detail how other derivatives of CDDO may affect general cell migration.

EXPERIMENTAL PROCEDURES

Cell Culture, Antibodies, and Reagents—Rat2 fibroblasts were cultured in a 37 °C incubator with 5% CO_2, and Dulbecco's modified Eagle's medium (DMEM) with 10% fetal bovine serum (FBS). Alexa Fluor 555-conjugated phalloidin (A34055) was purchased from Invitrogen. Monoclonal anti-Rac1 (610650) and anti-paxillin (610051) were purchased from BD Transduction Laboratories (Mississauga, Ontario). Monoclonal anti-β-tubulin (Tub2.1), anti-Arp3 (A5979), and polyclonal anti-actin (A2668) antibodies were purchased from Sigma. Monoclonal anti-cdc42 (sc8401) and polyclonal anti-RhoA (sc179), anti-n-WASp (sc-20770), and anti-GAPDH (sc-25778) antibodies were purchased from Santa Cruz Technology (Santa Cruz, CA). CDDO, CDDO-Im, CDDO-Me, biotinylated CDDO (b-CDDO), and biotinylated CDDO-Me (b-CDDO-Me) are generous gifts from Dr. M. B. Sporn (Hanover, NH). The biotinylated form of CDDO and CDDO-Me has been previously characterized and are referred to as compounds 5 and 6, respectively, by Honda and colleagues (50). The Arp3 inhibitor, CK-869, and the inactive control, CK-312, were purchased from Calbiochem.

Scratch Assays and Immunofluorescence Microscopy—Rat2 fibroblasts were grown to confluence, and the monolayer was scratched with a pipette tip. Cells were given 4 h to establish polarity and leading edges before being treated with 10 μM biotin, CDDO, CDDO-biotin, CDDO-Me, or CDDO-Me biotin for subcellular localization studies or with DMSO (vehicle) or CDDO, CDDO-Im, or CDDO-Me for 2 h for cell migration studies and immunofluorescence microscopy. For biotinylated subcellular localization studies, cells were fixed and permeabilized followed by incubation with anti-Rac1 antibody to visualize the leading edge. Cy2-labeled secondary antibodies, Cy3-labeled streptavidin antibody, and DAPI were then used to visualize Rac1, biotinylated CDDO, or biotinylated CDDO-Me and the nuclei of cells, respectively. Cells were visualized using an Olympus IX81 inverted microscope. For cell migration studies, DIC images were collected using an Olympus IX81 inverted microscope at the beginning of the experiment (time 0) and after 12–16 h. The extent of cell migration was measured by taking the width of the wound at time 0 and 16 h six times in duplicate. The results were averaged from four different experiments ± S.D. Statistical analyses were done using one-way analysis of variance. For immunofluorescence microscopy studies, cells were fixed, permeabilized, and incubated with anti-Arp3, anti-n-WASp, anti-actin, and anti-paxillin antibodies and phalloidin for stress fibers. Visualization was carried out using an Olympus IX81 inverted microscope. Micrograph deconvolution was carried out using ImagePro software (Media Cybernetics Inc.). Quantitative analysis for immunofluorescence studies were done as described previously (49).

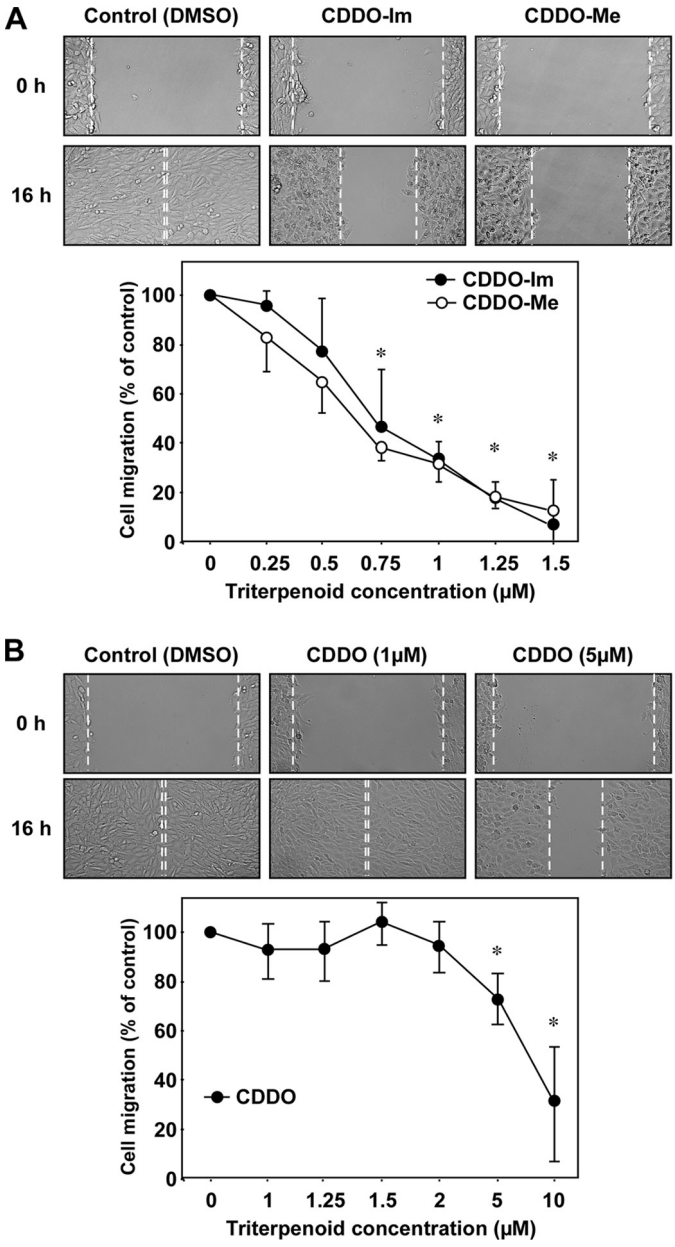

FIGURE 1. **CDDO-Im and CDDO-Me inhibit cell migration.** *A*, confluent Rat2 fibroblasts were scratched to create a wound and treated with 1 μM CDDO, CDDO-Im, or CDDO-Me for 16 h. Brightfield images (×10 magnification) were taken at the beginning of the experiment (*0 h*) and after 16 h (*16 h*) of incubation at 37 °C. The *white dotted lines* indicate the leading edge of migrating cells (*top panels*). Cells were treated with increasing concentrations of CDDO-Im or CDDO-Me (0–1.5 μM, as shown) and imaged. Cell migration was quantified using ImagePro software and graphed as cell migration (percentage of control) *versus* triterpenoid concentration ($n = 3 \pm$ S.D.). *, $p < 0.05$ (*bottom panel*). *B*, confluent Rat2 fibroblasts were scratched and incubated with DMSO (*Control*), or 1 or 5 μM CDDO (*top panels*). Cells treated with increasing concentrations of CDDO (0–10 μM, as shown) and imaged. Cell migration was quantitated as described in *panel A* and graphed as cell migration (percentage of control) *versus* triterpenoid concentration ($n = 3 \pm$ S.D.). *, $p < 0.05$.

Affinity Pulldown Using Biotinylated CDDO Derivatives—Subconfluent Rat2 fibroblasts or 2.5 μg of purified Arp2/3 complex protein were incubated with vehicle (DMSO), 10 μM biotin, or 10 μM b-CDDO or 10 μM b-CDDO-Me for 2 h before lysis, followed by incubation of neutravidin-agarose beads to precipitate proteins that associated with the biotinylated form of the synthetic triterpenoids. SDS-PAGE and silver staining were performed and proteins that were uniquely stained in biotinylated CDDO, and biotinylated CDDO-Me-treated samples were excised from the gel, trypsinized, and analyzed by electrospray mass spectrometry (ESI-MS). This approach was repeated three times. To confirm or identify the potential synthetic triterpenoid-binding proteins, lysates were processed for SDS-PAGE followed by immunoblotting with anti-tubulin, anti-actin, anti-Rac1, anti-Arp3, anti-Cdc42, or anti-RhoA antibodies.

Invitrogen™ Protoarray—The identification of triterpenoid-binding proteins was done by following the protocol described in the Invitrogen Protoarrray kit. Biotin or biotinylated CDDO-Me were incubated with a protein chip with about 8,000 human proteins spotted on a nitrocellulose membrane in duplicate for 2 h before incubating with streptavidin-Cy3 secondary antibody. The chip was then washed and dried before being read by the Bio-Rad VersArray ChipReader 3m system. Data were normalized against background and only signals that were at least 2-fold or more than the background were considered to be potential interacting candidates of the synthetic triterpenoids.

Small Rho GTPases Activation Assays—Subconfluent Rat2 fibroblasts were serum starved overnight before treating with vehicle (DMSO) or CDDO-Im for 2 h. For Rac1 and Cdc42 activation assays, cells were lysed and incubated with purified GST protein, or GST-PAK for 2 h before being processed for SDS-PAGE and immunoblotted for acti-

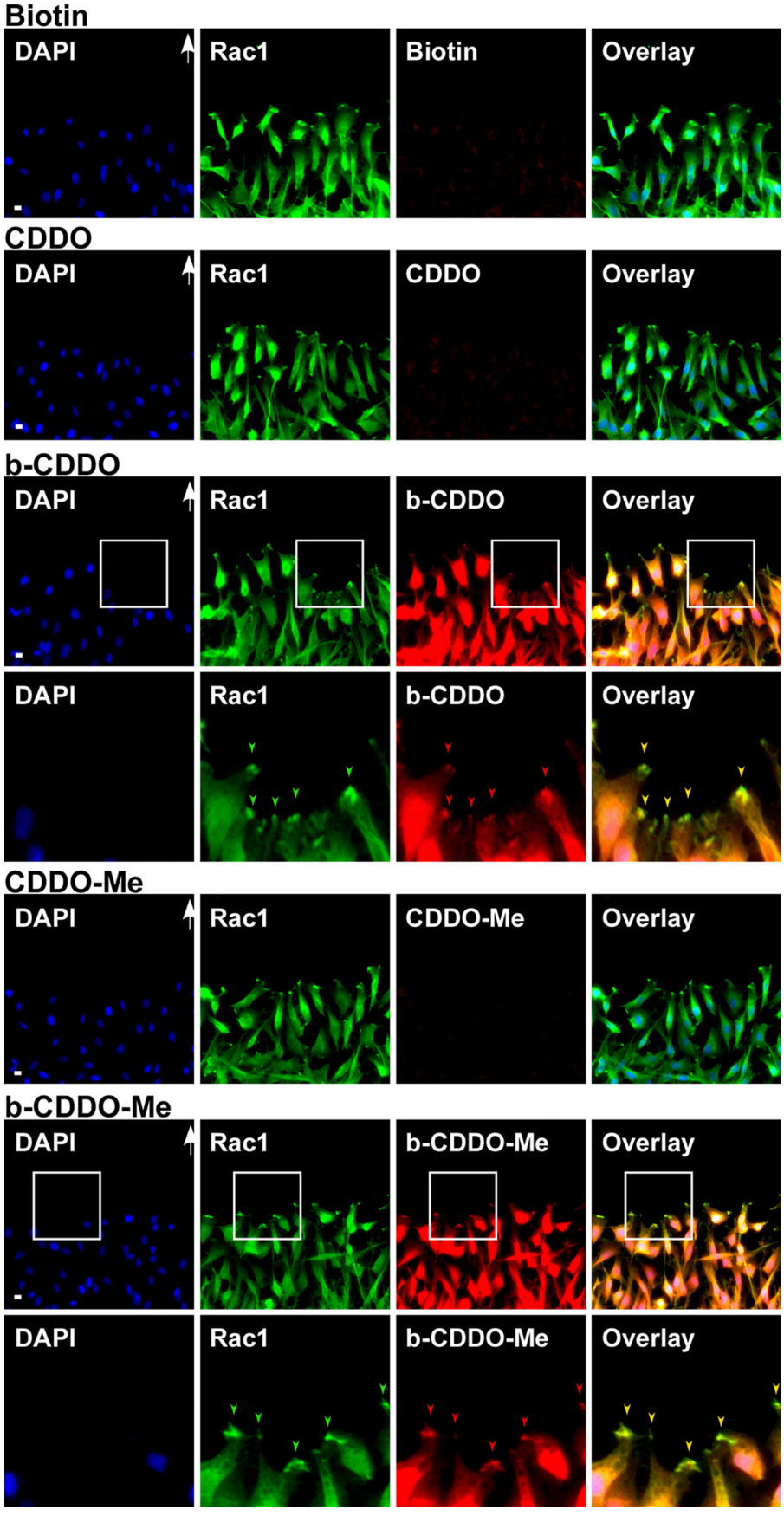

vated Rac1 and activated Cdc42 using anti-Rac1 and anti-Cdc42 antibodies, respectively. For RhoA activation assays, cells were lysed and incubated with purified GST or GST-Rhotekin for 2 h before being processed by SDS-PAGE and immunoblotted for activated RhoA using RhoA antibody. Total protein lysates were also immunoblotted and shown. Quantitative analyses were done using densitometry (Bio-Rad VersaDoc).

In Vitro Actin Polymerization Assays—Purified pyrene-labeled actin was resuspended and incubated in general actin buffer provided by the Cytoskeleton Inc. Actin Polymerization Kit for 1 h on ice to depolymerize any actin oligomers followed by microcentrifugation at 4 °C for 30 min. Two μM actin alone or 2 μM actin, 13 nM Arp2/3 complexes, and 100 nM VCA domain of WASp protein were incubated with DMSO (control) or different concentrations (0, 50, and 100 μM) of CDDO-Im and CDDO-Me for 15 min on ice before pyrene actin fluorescence was measured over time.

Docking Experiments—AutoDock version 4.2 was used to carry out the docking experiments (51). The crystal structures of the Arp2 and Arp3 subunits (PDB code 3DXM (52)) were used for the docking procedure, with the docking surface encompassing the interface between the two subunits as well as all of the internal cavities. The structure of CDDO-Me was obtained from the Cambridge Structural Data base (CSD-ID UFEHOC (53)). The CDDO-Im structure was constructed by merging the CDDO-Me structure with a suitable imidazole-containing compound (CSD-ID HEWQOQ). Both CDDO-Me and CDDO-Im are mostly rigid structures. For CDDO-Me, only the C17–C28 bond (which attaches the acid ester to the triterpenoid) was allowed to rotate; for CDDO-Im, both the C17–C28 bond and the bond between C28 and the imidazole nitrogen were rotatable. All other bonds in CDDO-Me and CDDO-Im were fixed, as was the structure of the Arp2 and Arp3 complex. The rigidity of CDDO-Me and CDDO-Im aided the docking procedure and also limited the number of potential solutions.

Competitive Binding Studies—Arp2/3 protein complex (2.5 μg) was incubated with either DMSO or increasing concentrations (10–100 μM) of CDDO-Me or CK-869 for 15 min at 37 °C. Following incubation with 10 μM b-CDDO-Me for an additional 15 min, 50% neutravidin-agarose beads were added and incubated at room temperature for 10 min. The beads were washed three times with TNTE buffer and subjected to SDS-PAGE and immunoblotting for Arp3.

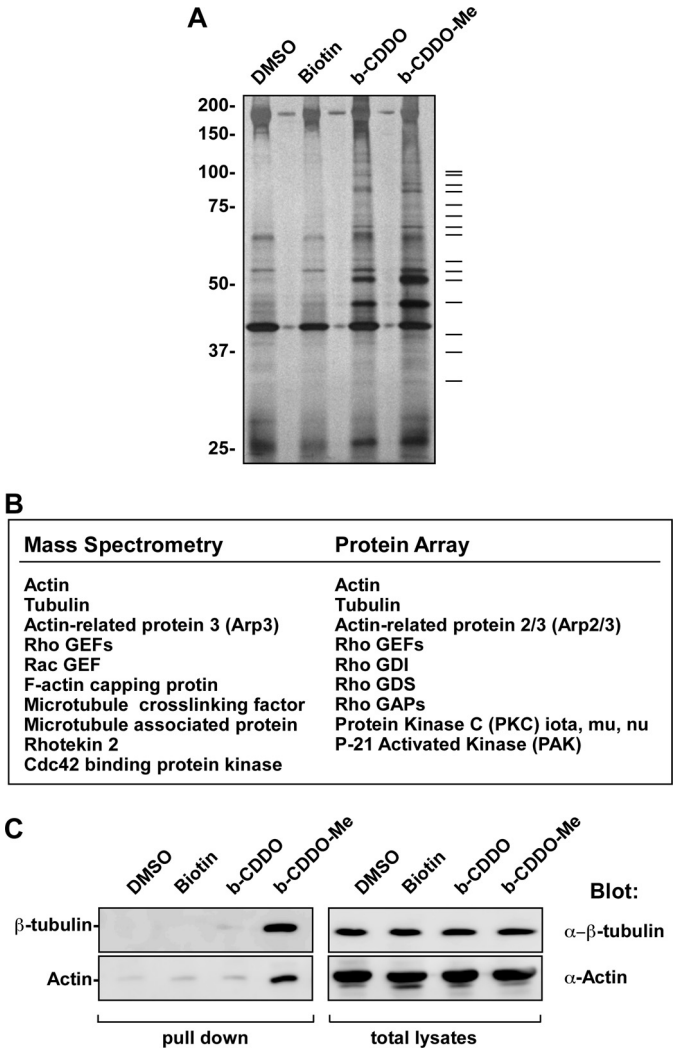

FIGURE 3. **Identification of triterpenoid-binding proteins.** *A*, Rat2 fibroblasts were incubated with DMSO, 10 μM biotin, 10 μM biotinylated-CDDO, or 10 μM biotinylated CDDO-Me, lysed, and incubated with neutravidin-agarose beads. SDS-PAGE and silver staining were performed and proteins that were uniquely stained in biotinylated CDDO-Me-treated samples were excised from the gel, trypsinized, and analyzed by electrospray mass spectrometry. *B*, summarized table of cell migration-related proteins from mass spectrometry and protein array approaches. *C*, Rat2 fibroblasts were incubated with DMSO, 10 μM biotin, 10 μM b-CDDO, or 10 μM b-CDDO-Me, lysed, and incubated with neutravidin-agarose beads. Precipitated samples (*left panels*) were processed by SDS-PAGE and immunoblotted for cytoskeletal proteins (anti-β-tubulin and anti-actin). Fifty micrograms of total protein lysates were also immunoblotted for tubulin and actin and shown (*right panel*).

RESULTS

We have shown that CDDO-Im inhibits cell migration and causes the disruption of the microtubule network through a mechanism distinct from microtubule-depolymerizing agents such as nocodazole (49). However, the molecular target(s) of this inhibition remain(s) unknown and we sought to identify them through the use of mass spectrometry and protein array analyses. For these techniques, we opted to use biotinylated synthetic triterpenoids that could be used for the purification and identification of associated proteins. Because the active nature of the imidazolide side group of CDDO-Im complicated its biotinylation, we used the CDDO and the methyl ester derivative (CDDO-Me) in our studies. CDDO-Me is a suitable substitute as it has been shown to be as potent as the CDDO-Im in

FIGURE 2. **b-CDDO and b-CDDO-Me target the leading edge of migrating cells.** Confluent Rat2 fibroblasts were scratched to create a wound. After incubation for 4 h to allow cell polarization and migration, cells were fixed, permeabilized, and incubated with monoclonal anti-Rac1 antibodies (Rac1; *green*) and biotin, CDDO, biotinylated CDDO (b-CDDO), CDDO-Me, or biotinylated CDDO-Me (b-CDDO-Me) followed by Cy2-labeled anti-mouse antibody and Cy3-labeled streptavidin. Cell nuclei were stained with DAPI (*blue*). The co-localization of Rac1 (*green*) with b-CDDO or b-CDDO-Me (*red*) at the leading edge of migrating cells is indicated (*yellow arrowheads*). The *white arrow* indicates the direction of cell movement. Representative images from four experiments are shown. *Bar* = 10 μm.

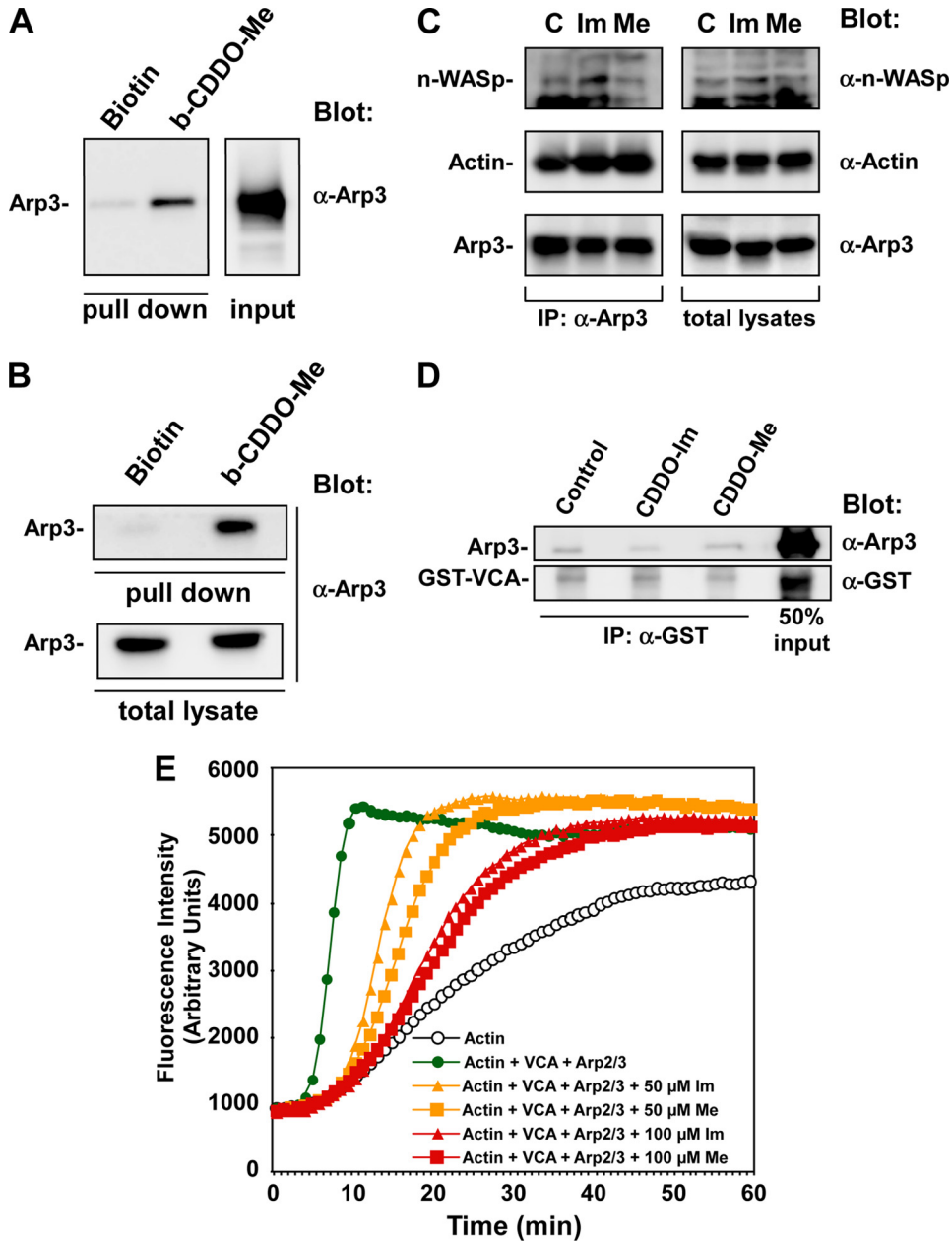

FIGURE 4. **Synthetic tritepenoids interact with the Arp2/3 and inhibit branched actin polymerization.** *A*, purified Arp2/3 protein complex (2.5 μg) was incubated with 10 μM biotin or 10 μM b-CDDO-Me for 2 h. An affinity pulldown assay was performed by incubating samples with neutravidin beads for 1 h followed by SDS-PAGE and immunoblotting with anti-Arp3 antibodies (*left panel*). Total input was also immunoblotted with Arp3 and shown (*right panel*). *B*, Rat2 fibroblasts were incubated with 10 μM biotin or b-CDDO-Me for 2 h before lysis, followed by incubation of streptavidin-agarose beads to precipitate proteins that associated with the biotinylated form of the synthetic triterpenoids. SDS-PAGE was performed followed by immunoblotting for Arp3 with anti-Arp3 antibody (*top panel*). Fifty μg of protein lysates were also immunoblotted for Arp3 and shown (*bottom panel*). *C*, subconfluent Rat2 fibroblasts were treated with DMSO (Control; *C*), 1 μM CDDO-Im (*Im*), or 1 μM CDDO-Me (*Me*) for 2 h before lysis followed by immunoprecipitation with anti-Arp3 antibody. The immunoprecipitates (*IP*; *left panel*) were then subjected to SDS-PAGE and immunoblotting with anti-n-WASp, anti-actin, and anti-Arp3 antibodies. Fifty micrograms of total lysates were also immunoblotted for n-WASp, actin, and Arp3 and shown (*right panel*). Note that the association of Arp3 and n-WASp is not altered by triterpenoid treatment. *D*, purified Arp2/3 complex and the GST-VCA domain of nWASp were incubated in the absence or presence of triterpenoids and immunoprecipitated with anti-GST antibodies. The immunoprecipitates (*IP*; *left panel*) were then subjected to SDS-PAGE and immunoblotting with anti-GST and anti-Arp3 antibodies. Fifty percent of the input was also immunoblotted for GST and Arp3 and shown (*right*). Note that the association of Arp3 and n-WASp is not altered by triterpenoid treatment. *E*, purified pyrene-labeled actin was incubated for 1 h on ice to depolymerize actin oligomers. Two μM actin (Actin) or actin in the presence of 13 μM Arp2/3 complex (Arp2/3) and 100 nM VCA domain of n-WASp protein (*VCA*) were incubated with DMSO, 50 or 100 μM of either CDDO-Im (*Im*) or CDDO-Me (*Me*). Actin polymerization was measured by pyrene fluorescence and graphed as fluorescence intensity (arbitrary units) *versus* time (min).

many cellular assays (7, 13, 17, 24, 54), compared with the weaker CDDO parental compound.

Synthetic Triterpenoids Inhibit Cell Migration and Localize to the Leading Edge of Migrating Cells—We first set out to establish the effectiveness of the CDDO-Me compound in cell migration by comparing its rate of cell migration with CDDO- and CDDO-Im-treated cells (Fig. 1). Briefly, Rat2 fibroblasts were grown to confluence before a "wound" was created by scratching the cells off of the surface of the culture dish. The cells were treated with varying concentrations of synthetic triterpenoids (Fig. 1). Brightfield images were taken at zero time and again after 16 h of incubation at 37 °C to examine whether the rate of cell migration would be affected by CDDO, CDDO-Im, and CDDO-Me (Fig. 1). We observed that cell migration remained relatively unaltered in the presence of 1 μM CDDO, whereas cell migration was inhibited >50% in the presence of either 1 μM CDDO-Im or CDDO-Me (Fig. 1). Indeed, at 1.5 μM, the rate of cell migration in CDDO-Im- and CDDO-Me-treated cells was reduced to 80%, whereas the rate of migration in CDDO-treated cells did not differ from control. Compared with the imidazolide and methyl ester derivatives, the parental CDDO is inactive at 1 μM in inhibiting cell migration and was used as a inactive control in subsequent studies. To address cell toxicity, the drugs were washed out using PBS and the cells were incubated with medium for an additional 24 h. We observed that cells incubated with <5 μM CDDO and ≤1.25 μM CDDO-Im and CDDO-Me migrated and filled the wound (data not shown). This further confirmed that CDDO is ~10 times less potent than the CDDO-Im and -Me derivatives. These more potent triterpenoids also acted in similar concentration ranges to reduce cell migration.

We previously demonstrated that CDDO localizes to the leading edge of migrating cells (49) and may tar-

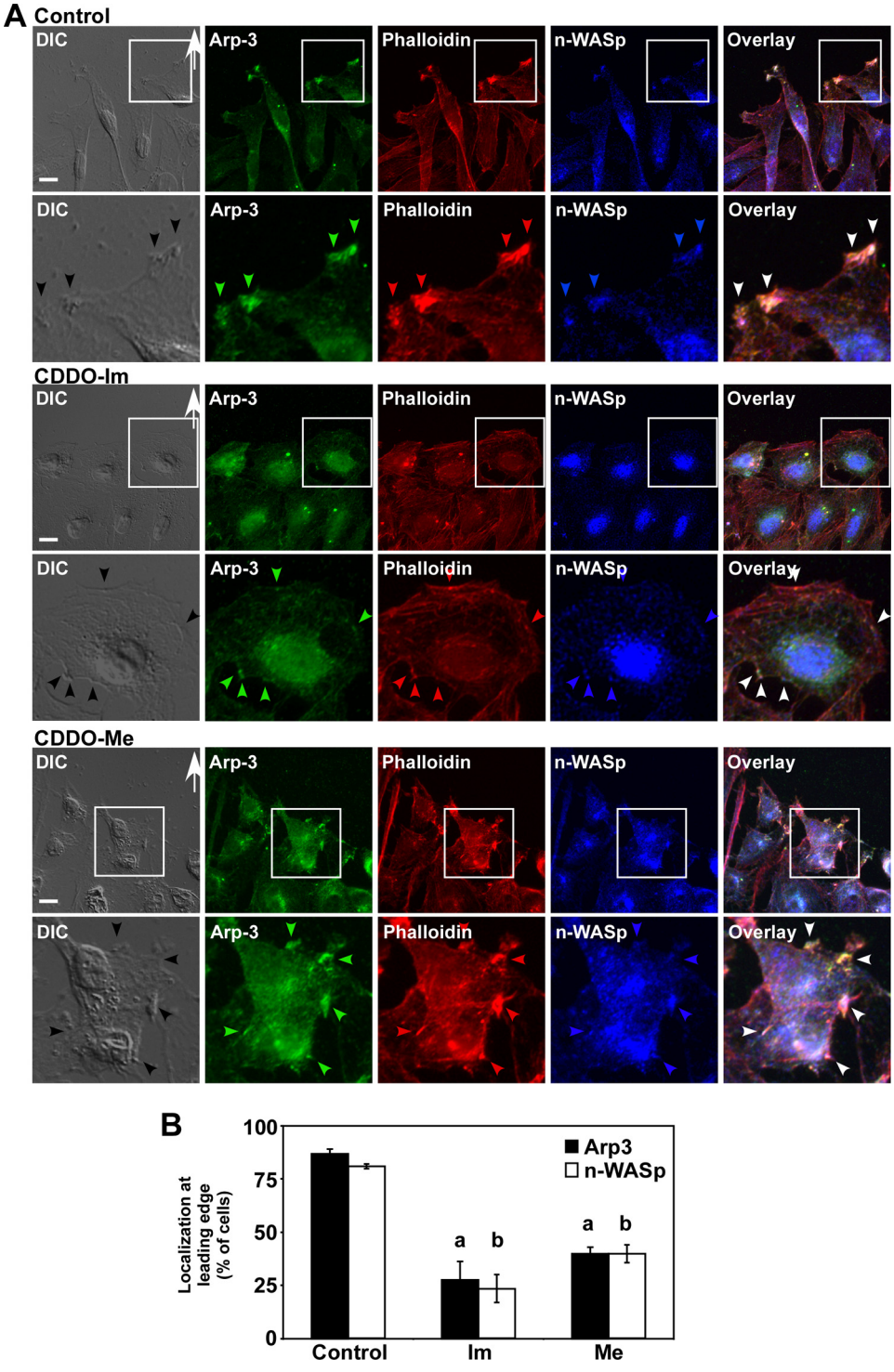

FIGURE 5. **Synthetic triterpenoids affect the localization of Arp3 and n-WASp at the leading edge of polarized cells.** *A*, Rat2 fibroblasts were scratched and incubated for 4 h at 37 °C to establish cell polarity and then treated with control medium (Control; *top*), 1 μM CDDO-Im (CDDO-Im; *middle panel*), or 1 μM CDDO-Me (CDDO-Me; *bottom panel*) for an additional 2 h. The cells were then fixed, permeabilized, and immunostained with anti-Arp-3 (Arp3; *green*), phalloidin for stress fibers (Phalloidin; *red*), and anti-n-WASp (n-WASp; *blue*) antibodies. The scratches were made in the horizontal plane *above* the cells. Arp-3, actin, and n-WASp proteins at the leading edge of migrating cells are indicated by *green*, *red*, and *blue arrowheads*, respectively. The *white arrowheads* indicate the co-localization of all three proteins. *White arrows* indicate the direction of cellular movement. DIC microscopy was included to visualize the leading edge of migrating cells. *Bar* = 10 μm. *B*, quantitation of cells containing Arp-3 or n-WASp at the leading edge of migrating cells was carried out using ImagePro software and graphed as localization at the leading edge (% of cells) *versus* treatment ($n = 3 \pm$ S.D.). *a* and *b*, $p < 0.05$ of Arp3 and nWASp, compared with respective controls.

get proteins involved in the polarity complex at this cellular locus. We therefore assessed if CDDO-Me also targets the leading edge of migrating cells using immunofluorescence microscopy. We observed that b-CDDO-Me localizes to the leading edge of migrating cells, similar to biotinylated CDDO (Fig. 2). These results demonstrate that the subcellular localization of CDDO and CDDO-Me is similar.

Identification of Triterpenoid-binding Proteins—Because CDDO-Im and CDDO-Me exhibited similarities in cellular localization and inhibition of cell migration, we used b-CDDO-Me to identify potential synthetic triterpenoid targets using two proteomic approaches (Fig. 3). In the first approach, we utilized a mass spectrometry-based method and proteins that precipitated with b-CDDO or b-CDDO-Me were processed by SDS-PAGE followed by silver staining and trypsinization before being sent for ESI-MS analysis (Fig. 3*A*). This mass spectrometry method was compared with a protein array approach, which was purchased from Invitrogen. The slide, containing >8000 human purified proteins, was incubated with biotin, biotinylated CDDO, or biotinylated CDDO-Me followed by Alexa Fluor 647-labeled streptavidin. The triterpenoid-binding proteins were then visualized and proteins that bound the biotinylated-CDDO-Me ≥2-fold higher than biotin alone were counted as potential triterpenoid-binding targets (data not shown). Using two different proteomic approaches and by comparative analysis, several proteins involved in cytoskeletal organization and cell migration were identified (Fig. 3*B*).

To ascertain that the identified binding partners are also *bona fide* cellular interacting proteins, we incubated cells with b-CDDO or b-CDDO-Me, lysed the cells, and precipitated b-CDDO or b-CDDO-Me with neutravidin beads and Western blotted the precipitates with antibodies against tubulin and actin (Fig. 3*C*). Consistent with pre-

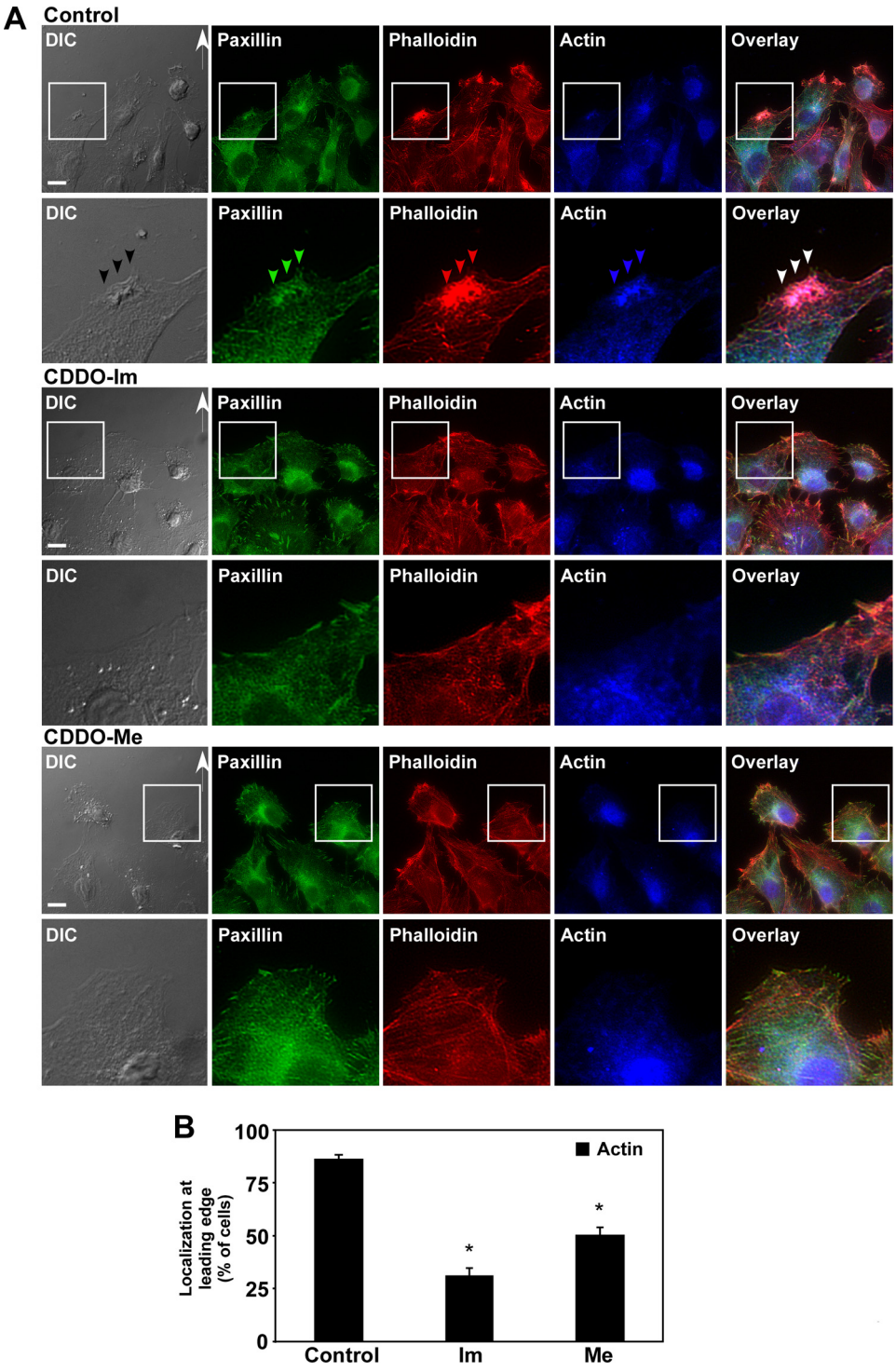

FIGURE 6. **CDDO-Im and CDDO-Me do not affect stress fibers or focal adhesions but reduce branched actin at the leading edge of migrating cells.** *A*, Rat2 fibroblasts were scratched and incubated for 4 h at 37 °C to establish cell polarity and then treated with control medium (*Control*; *top*), 1 μM CDDO-Im (*middle panel*), or 1 μM CDDO-Me (*bottom panel*) for an additional 2 h. The cells were then fixed, permeabilized, and immunostained with anti-paxillin (paxillin; *green*), phalloidin for stress fibers (phalloidin; *red*), and anti-actin (actin; *blue*) antibodies. The scratches were made in the horizontal plane *above* the cells shown and the leading edge of migrating cells containing paxillin, stress fibers, and actin were indicated by *green*, *red*, and *blue arrowheads*, respectively. The *white arrowheads* indicate co-localization and the *white arrows* indicate the direction of cellular movement. DIC microscopy was included to visualize the leading edges of migrating cells. *Bar* = 10 μm. *B*, quantitation of cells containing actin at the leading edge of migrating cells was carried out using ImagePro software and graphed as localization at the leading edge (% of cells) *versus* treatment ($n = 3 \pm$ S.D.). *, $p < 0.05$.

viously published results (55), we found that tubulin interacts with the b-CDDO-Me and was also detected to interact with b-CDDO, albeit to a much lower extent. Interestingly, actin, a large component of the cytoskeleton, and actin-related protein 3 (Arp3), were also found to associate with b-CDDO-Me (Figs. 3*C* and 4*A*).

Another group of proteins identified in our proteomic approaches were modulators of the Rho GTPase family (Fig. 3*B*). Rho GTPases are a group of G-proteins extensively involved in the establishment of cell polarity and orientation of the cytoskeletal dynamics during cell migration. They are regulated by guanine exchange factors, which promote the activation of small Rho GTPases, and by GTPase activating proteins, which render the protein into its inactive state.

The possibility that triterpenoids affect the activity of one or more of the numerous guanine exchange factor and GTPase activating proteins (56) was assessed by directly testing the GTP-bound state of Rac1, RhoA, or Cdc42. We observed that CDDO-Im only moderately increased Rac1 activity but was ineffective in altering Cdc42 and RhoA activities (supplemental Fig. S1, *A* and *B*). In addition, affinity pull-down assays using specific antibodies against Rac1, Cdc42, and RhoA indicated that b-CDDO-Me does not bind to these small GTPases (supplemental Fig. 1*C*).

CDDO-Im and CDDO-Me Inhibit Branched Actin Polymerization by Targeting Arp3—We next directed our attention to molecules that are downstream of GTPases and alter the cytoskeleton and cell migration: molecules that alter the actin cytoskeleton. There are two different actin assembly machineries involved in the formation of actin with different properties in different areas of migrating cells. Arp2/3 complex is involved in the assembly of branched actin at the leading edge of migrating cells, whereas formin is involved in the formation of unbranched actin such as stress fibers

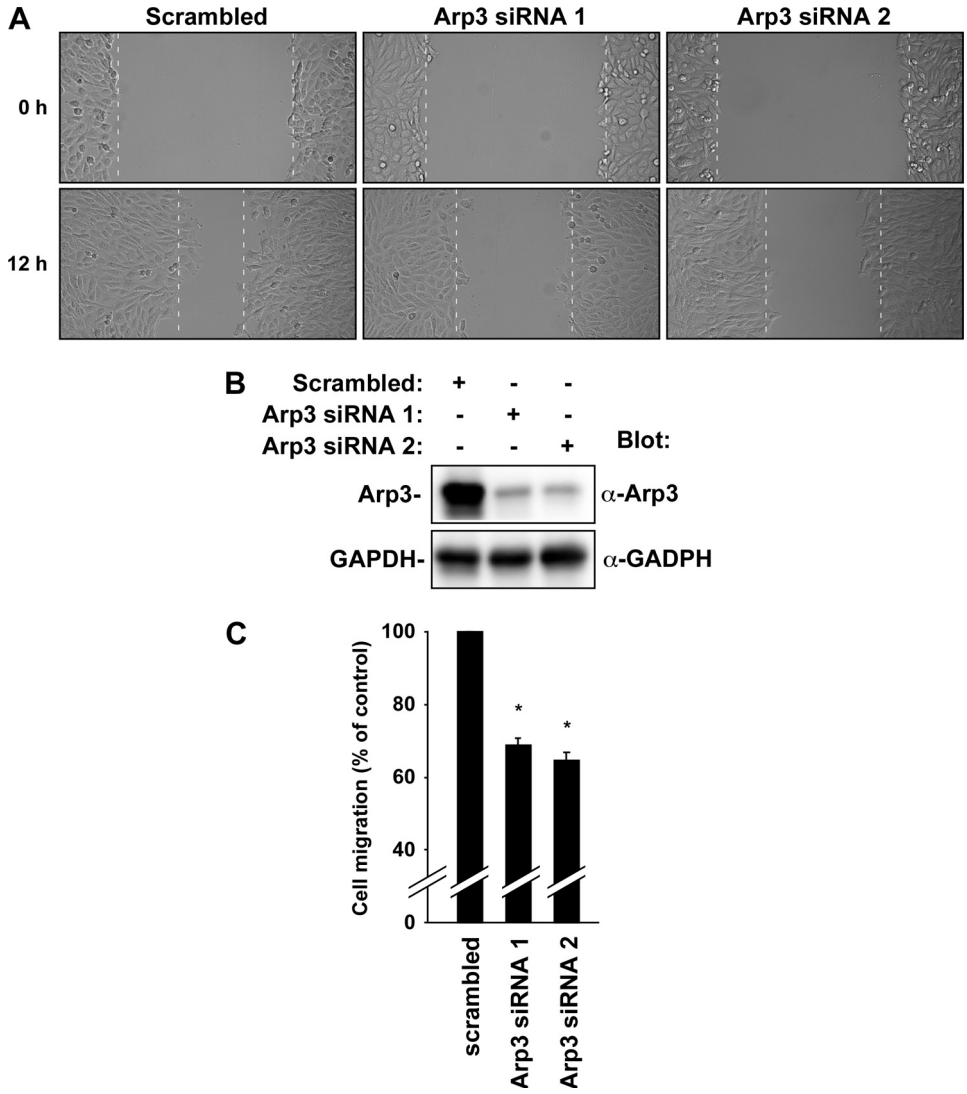

FIGURE 7. **Silencing Arp3 expression reduces cell migration.** *A*, Rat2 fibroblasts were transfected with control siRNA (*scrambled*), or two siRNA specific for Arp3 (*Arp3 siRNA 1* and *2*). When the cells reached confluence, they were scratched to create a wound. Brightfield images (×10 magnification) were taken at the beginning of the experiment (*0h*) and after 12 h (*12h*) of incubation at 37 °C. The *white dotted lines* indicate the edge of the leading edge of migrating cells. *B*, representative immunoblots of the cells described in *panel A* probed with Arp3 antibodies (*top panel*) or GAPDH (*bottom panel*). *C*, quantitation of cell migration described in *panel A* was carried out using ImagePro software and graphed as cell migration (percentage of control) *versus* siRNA treatment ($n = 3 \pm$ S.D.). *, $p < 0.05$.

(3). We have previously observed that the actin stress fibers are largely unaffected by triterpenoid treatment (49), so we examined whether synthetic triterpenoids have any effect on branched actin formation by studying actin and Arp2/3 complex.

Arp2/3 is a stable complex composed of five subunits: ARPC1, ARPC2, ARPC3, ARPC4, and ARPC5 and two actin-related proteins Arp2 and Arp3. In particular, studies have shown that Arp3 is involved in the nucleation process of branched actin formation (3). We first attempted to confirm whether Arp3 was a direct target of the synthetic triterpenoid through affinity pulldown assays by using both purified Arp2/3 complex protein as well as in Rat2 cells (Fig. 4). Briefly, Apr2/3-purified protein was incubated with DMSO (control), biotin, biotinylated CDDO, or biotinylated CDDO-Me for 2 h and precipitated with neutravidin beads followed by immunoblotting with anti-Arp3 antibody. Our results showed that Arp3 interacted with CDDO-Me *in vitro* (Fig. 4*A*). To confirm this interaction in cells, we incubated Rat2 fibroblasts with b-CDDO-Me, precipitated, and immunoblotted for Arp3 (Fig. 4*B*). These two approaches confirmed our proteomic analyses and indicate that Arp3 associates with triterpenoids.

For the formation of branched actin to occur, Arp2/3 must interact and work closely with not only actin itself, but also n-WASp. Indeed, n-WASp regulates cytoskeletal dynamics by activating Arp2/3 complexes so that it can begin the nucleation process for branched actin polymerization. Therefore, we hypothesize that the triterpenoid may inhibit cell migration by targeting Arp3 directly and affecting the association of Arp3 with actin and/or n-WASp. To assess this, co-immunoprecipitation assays were done using Rat2 fibroblasts. Cells were treated with DMSO, 1 μM CDDO-Im or CDDO-Me, immunoprecipitated with anti-Arp3 antibody, and immunoblotted for actin, n-WASp, and Arp3 antibodies. Results showed that Arp3 remained associated with both n-WASp and actin upon CDDO-Im or CDDO-Me incubation (Fig. 4*C*). These results suggest that the association between Arp3 and n-WASp is unaffected by the synthetic triterpenoids in cells or *in vitro* (Fig. 4*D*).

The identification that subunits of the Arp2/3 complex are direct triterpenoid-binding proteins next led us to study the effect of branched actin polymerization in the presence of CDDO-Im and CDDO-Me. We examined the rate of actin polymerization in the presence of actin alone or actin and the VCA domain of n-WASp and Arp2/3, in the absence or presence of different concentrations of CDDO-Im and CDDO-Me (Fig. 4*E*). We observed that the rate of actin polymerization was reduced by both CDDO-Me and CDDO-Im, with 50 μM of either compound effectively reducing the rate of actin polymerization by about 50%. At 100 μM, both triterpenoids were able to greatly reduce Arp2/3/VCA-dependent actin polymerization but did not alter actin polymerization in the absence of Arp2/3-VCA (Fig. 4*E* and data not shown). Our results suggest that triterpenoids target Arp2/3/n-WASp-mediated branched actin polymerization.

We then assessed whether the cellular localization of Arp3 was also affected by triterpenoid treatment (Fig. 5). Confluent Rat2 fibroblasts were scratched and cells were then allowed to

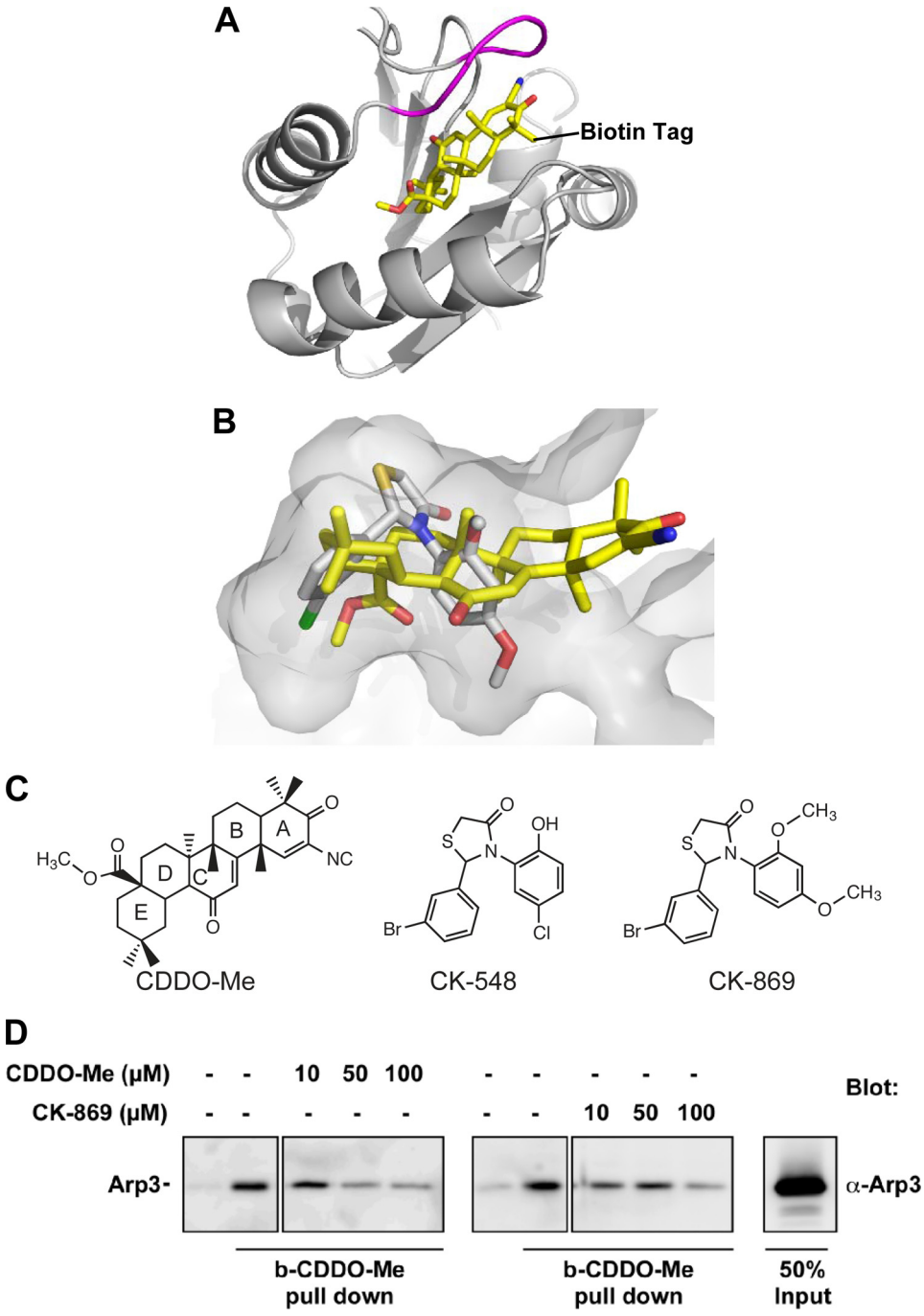

FIGURE 8. **Docking of CDDO-Me to the Arp2/3 complex.** The surface and internal cavities of the Arp2/3 complex (PDB code 3DXM (52)) were used to find low energy binding sites for CDDO-Me and CDDO-Im with the program Autodock (51). *A*, a hydrophobic pocket provided the lowest energy binding site for CDDO-Me; the same pocket is predicted to bind CDDO-Im in an identical position and orientation, but with even greater affinity (not shown). The pocket is formed by a β-sheet and two α-helices, with the methyl ester moiety of CDDO-Me buried deeply in the pocket. In this situation, the site of attachment for the biotin tag (which was not included in the docking experiments) is solvent exposed and accessible. Thus, the best binding site found by *in silico* docking is consistent with the biochemical experiments. In unliganded Arp3 structures, a loop comprising residues 79 to 84 (in *magenta*) closes over the hydrophobic pocket, blocking access to the site. The change in conformation of this loop represents the only structural difference associated with drug binding to the hydrophobic pocket (52). *B*, the internal surface of the hydrophobic pocket is *outlined*, with CDDO-Me in the low energy docked position. CK-869 is also shown in a docked position that is essentially identical to the position of CK-548 (not shown) in the crystal structure of the Arp2/3-CK-548 complex (52). CDDO-Me presents a greater contact surface and is much more rigid than CK-869, and its predicted affinity for Arp3 is higher. *C*, a comparison of the chemical structures of the three compounds used in the docking experiments; CK-548 was also co-crystallized with Arp3 (52). In docking experiments, both CK-548 and CK-869 were predicted to bind with highest affinity to the hydrophobic pocket, in an orientation and position that is virtually identical to that observed for CK-548 in the Arp3-CK-548 crystal structure (52). *D*, competitive binding of b-CDDO-Me with CK-869. Purified Arp2/3 complex (2.5 μg) was incubated with 10 μM biotinylated CDDO-Me in the absence or presence of increasing concentrations of CDDO-Me or CK-869 (10–100 μM). The biotin-CDDO-Me-bound Arp3 was precipitated with neutravidin beads, processed for SDS-PAGE, and immunoblotted with Arp3 antibodies. Fifty percent of the input was also blotted with Arp3 antibodies and shown on the *right*.

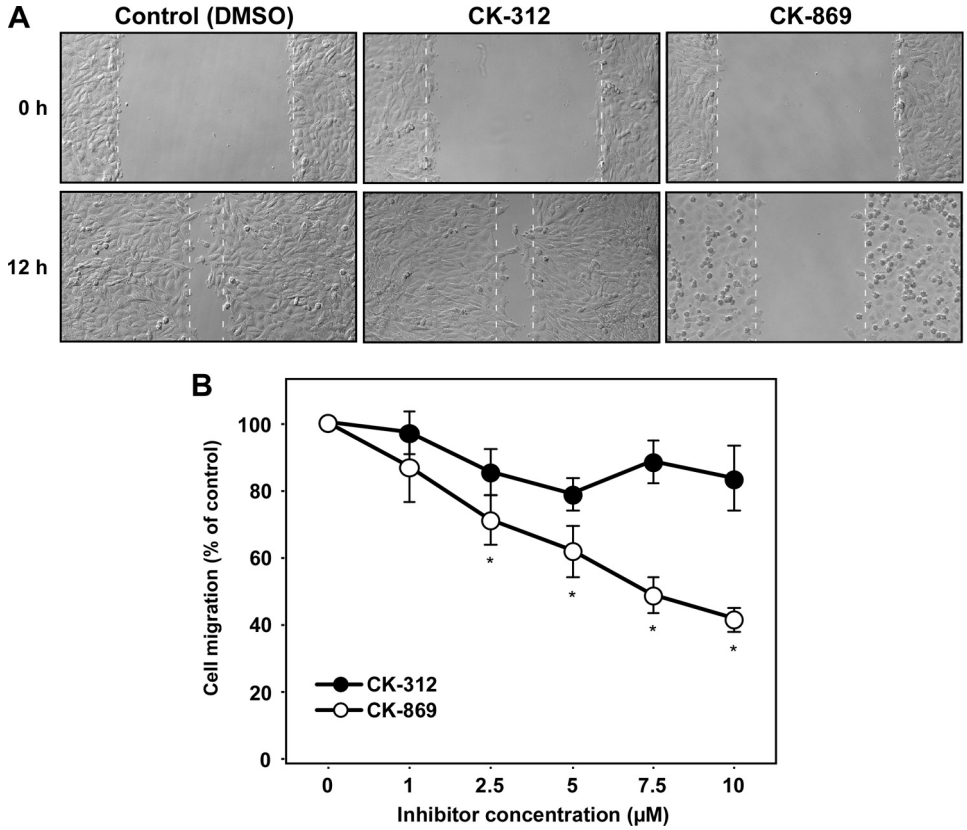

FIGURE 9. **CK-869 inhibits cell migration.** *A*, confluent Rat2 fibroblasts were scratched to create a wound and treated with DMSO (*Control*), 5 μM CK-312 (inactive control), or 5 μM CK-869 for 12 h. Brightfield images ($\times$10 magnification) were taken at the beginning of the experiment (*0 h*) and after 12 h (*12 h*) of incubation at 37 °C. The *white dotted lines* indicate the leading edge of migrating cells. *B*, cells were treated with increasing concentrations of CK-312 (inactive control) or CK-869 (1–10 μM) and imaged. Cell migration was quantified using ImagePro software and graphed as cell migration (percentage of control) *versus* Arp3 inhibitor concentration ($n = 3 \pm$ S.D.). *, $p < 0.05$.

polarize and establish a leading edge before being treated with DMSO, 1 μM CDDO-Im or CDDO-Me. The cells were then fixed, permeabilized, and stained for Arp3, n-WASp, and phalloidin. We observed that Arp3 and n-WASp co-localized at the leading edge of polarized cells in the absence of CDDO-Im; however, when treated with CDDO-Im, both proteins were displaced from the leading edge and appeared diffused throughout the cytoplasm of the cell (Fig. 5). CDDO-Me gave similar, albeit slightly reduced, effects as the CDDO-Im compound.

To confirm that the action of triterpenoids was specific to Arp3 and branched actin, we examined the effect of the synthetic triterpenoids on stress fibers and focal adhesions using immunofluorescence studies (Fig. 6). Stress fibers are one of the most common and indicative unbranched actin structures in the cell and paxillin is a marker of focal adhesions. Confluent Rat2 cells were scratched and treated with the synthetic triterpenoids for 2 h before fixation and permeabilization. Fluorescently tagged antibodies and phalloidin were used to stain for paxillin, stress fibers, and actin, respectively. We found that the structures of both stress fibers and focal adhesions were not diminished by CDDO-Im or CDDO-Me treatment (Fig. 6). However, consistent with our *in vitro* data, branched actin staining was reduced at the leading edge of migrating cells after the incubation with triterpenoids (Fig. 6*B*).

Having observed that triterpenoids inhibit Arp2/3 activity and branched actin formation, we next assessed if knockdown of the Arp3 protein would inhibit Rat2 cell migration (Fig. 7). We observed that a 65–70% silencing of Arp3 protein levels (Fig. 7*B*), reduced Rat2 cell migration by ~35% (Fig. 7*C*).

These results suggest that the inhibition of Arp3 activity may be a mechanism whereby triterpenoids inhibit cell migration. To lend additional support for this hypothesis, we used *in silico* docking to identify potential high affinity triterpenoid binding sites in Arp3.

Identification of a CDDO-Me-binding Site on Arp3—To put our observations in the context of the recently characterized Arp2/3 inhibitors (52), docking experiments were carried out using the crystal structures of Arp2/3 (PDB code 3DXM (52)). The structure used for the docking experiments had been solved with a small molecule inhibitor, CK-548, bound to a hydrophobic pocket in Arp3. We tested the docking procedure using this inhibitor. The two top solutions corresponded to binding of CK-548 in the same hydrophobic pocket, but in two different orientations, which were the same in terms of predicted interaction energy (−8.9 kcal/mol, corresponding to a K_I of 315 nM). One of these solutions was identical to the position and conformation observed in the Arp3-CK-548 crystal structure, validating the accuracy of the docking procedure. A closely related compound, CK-869, docked to an identical position, with a slightly higher predicted K_I of 460 nM. This docked position for CK-869 corresponded very closely to the model for the Arp3-CK-869 complex proposed by Pollard and co-workers (52).

Interestingly, we observed that the triterpenoid CDDO-Me docked to Arp3 in the same hydrophobic pocket (Fig. 8, *A* and *B*). The docked position shown in Fig. 8 has a binding energy of −13.3 kcal/mol and predicted K_I of 180 pM; this was the lowest energy solution obtained for the surface encompassing the Arp2 and Arp3 interface regions, including all of the internal cavities. CDDO-Im, which has an imidazole group attached to the acid in place of the methyl in CDDO-Me, docked to the same pocket on Arp3, but with an even higher predicted affinity (K_I of 27 pM). It is noteworthy that the lowest energy docked positions for both CDDO-Me and CDDO-Im exposes C23 of the triterpenoid to the solvent: this is the site of attachment for the biotin label used for isolating the Arp2/3 complex from Rat2 fibroblasts, and therefore the lowest energy docked position is fully consistent with binding of the biotinylated CDDO-Me derivative. As can be seen in Fig. 8*B*, the posi-

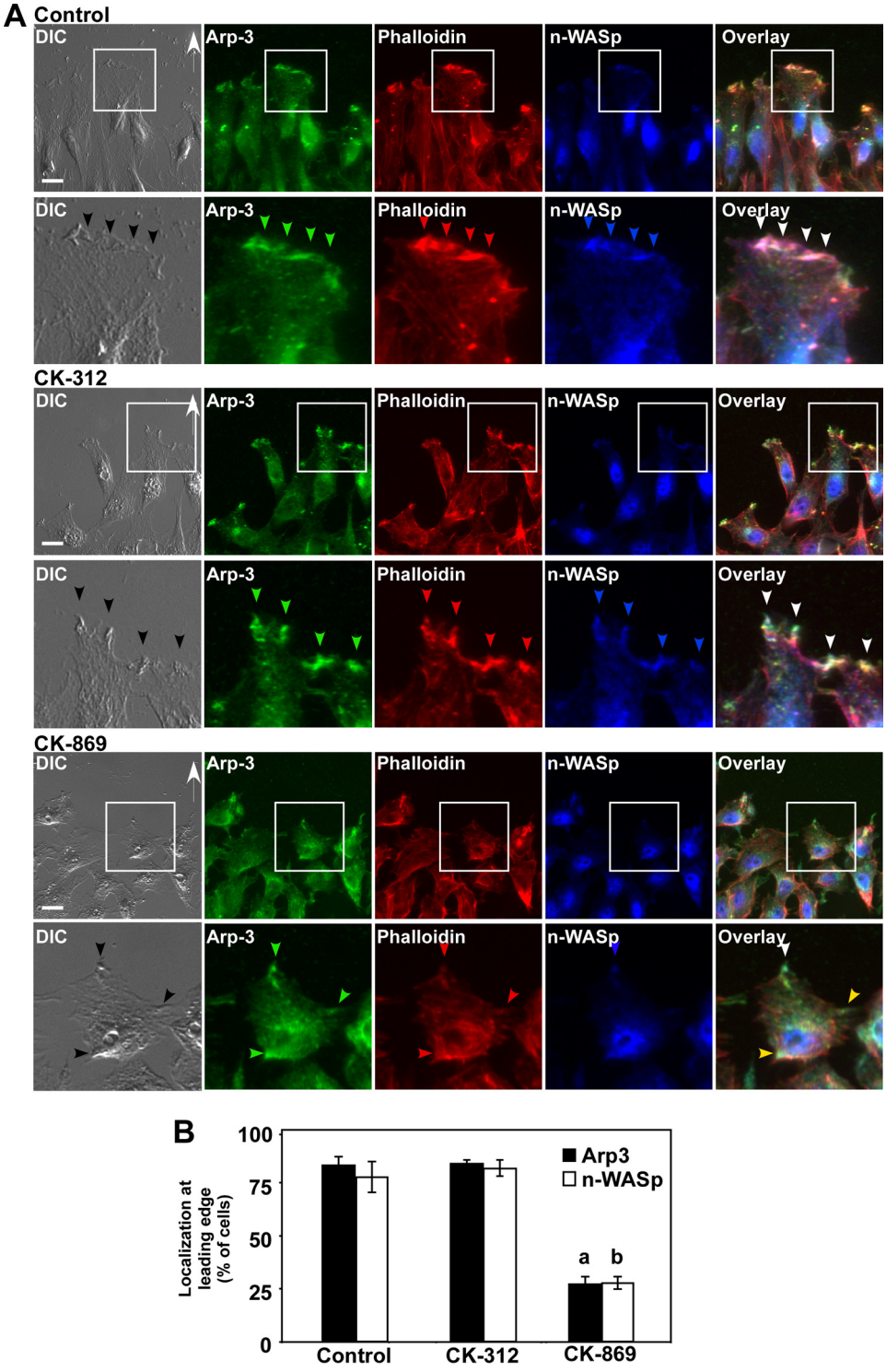

FIGURE 10. **CK-869 affects the localization of Arp3 and n-WASp at the leading edge of polarized cells.** *A*, Rat2 fibroblasts were scratched and incubated for 4 h at 37 °C to establish cell polarity and then treated with control medium (*Control*; *top*), 10 μM CK-312 (*middle panel*), or 10 μM CK-869 (*bottom panel*) for an additional 2 h. The cells were then fixed, permeabilized, and immunostained with anti-Arp-3 (Arp3; *green*), phalloidin for stress fibers (phalloidin; *red*), and anti-n-WASp (n-WASp; *blue*) antibodies. The scratches were made in the horizontal plane *above* the cells. Arp-3, actin, and n-WASp proteins at the leading edge of migrating cells are indicated by *green*, *red*, and *blue arrowheads*, respectively. The *white arrowheads* indicate the co-localization of all three proteins. *White arrows* indicate the direction of cellular movement. DIC microscopy was included to visualize the leading edge of migrating cells. *Bar* = 10 μm. *B*, quantitation of cells containing Arp-3 or n-WASp at the leading edge of migrating cells was carried out using ImagePro software and graphed as localization at the leading edge (% of cells) *versus* treatment ($n = 3 \pm$ S.D.). *a* and *b*, $p < 0.05$ of Arp3 and n-WASp, compared with respective controls.

tion that CDDO-Me is predicted to occupy matches closely to the docked position of CK-869, which in turn is virtually identical to the position of CK-548 in the actual crystal structure (52). Compared with unliganded Arp3 structures, both CDDO-Me and CDDO-Im require a localized conformation change in the loop comprising residues 79 to 84, which opens the pocket to allow binding (Fig. 8*A*). The much tighter predicted binding for CDDO-Me compared with CK-869 is consistent with the lower concentrations of CDDO-Me required for biological effects.

To confirm that CDDO-Me and CK-869 bind to the same site in Arp3, binding competition assays were carried out with CK-869 and non-biotinylated CDDO-Me as a control (Fig. 8*D*). With increasing concentrations of CDDO-Me or CK-869, the amount of Arp3 that precipitated with biotinylated-CDDO-Me was reduced (Fig. 8*D*). This is consistent with our docking analysis that indicates that CK-869 and CDDO-Me bind in the same hydrophobic pocket.

Inhibition of Arp3 Attenuates Cell Migration and Cell Polarity—To assess if the inhibition of Arp3 using CK-869 could also abrogate cell migration, we incubated cells with increasing concentrations of CK-869 (Fig. 9). We observed that 7.5 μM CK-869 was able to inhibit cell migration by 50% (Fig. 9*B*). The negative control, CK-312, which was characterized to bind to Arp3 but not inhibit its function, did not alter cell migration at the concentration range tested (Fig. 9*B*). An interesting observation of the cells treated with the CK-869 Arp3 inhibitor was that the cells adopted a rounded up morphology and gave the appearance of detaching. However, over time the cells flattened (supplemental Movie S1). This suggests that the cells may undergo cyclical rounding up and flattening in the presence of an Arp3 inhibitor.

Finally, we assessed if incubating polarized cells with CK-869 would affect branched actin polymerization in a manner similar to

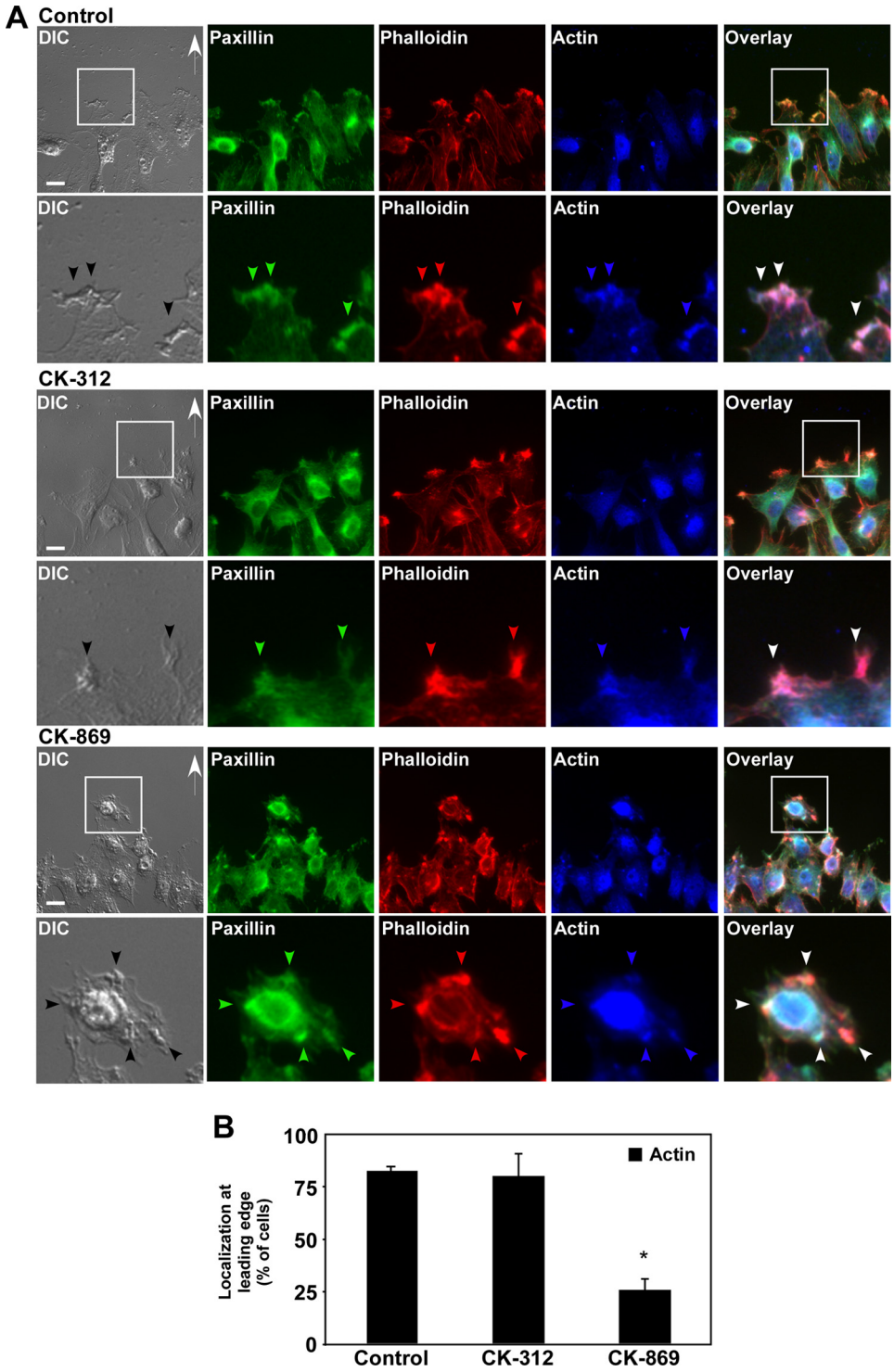

FIGURE 11. **CK-869 does not affect stress fibers or focal adhesions but reduces branched actin at the leading edge of migrating cells.** *A*, Rat2 fibroblasts were scratched and incubated for 4 h at 37 °C to establish cell polarity and then treated with control medium (*Control*; *top*), 10 μM CK-312 (*middle panel*), or 10 μM CK-869 (*bottom panel*) for an additional 2 h. The cells were then fixed, permeabilized, and immunostained with anti-paxillin (*green*), phalloidin for stress fibers (phalloidin; *red*), and anti-actin (*blue*) antibodies. The scratches were made in the horizontal plane *above* the cells. Paxillin, branched actin, and actin proteins at the leading edge of migrating cells are indicated by *green*, *red*, and *blue arrowheads*, respectively. The *white arrowheads* indicate the co-localization of all three proteins. *White arrows* indicate the direction of cellular movement. DIC microscopy was included to visualize the leading edge of migrating cells. *Bar* = 10 μm. *B*, quantitation of cells containing actin at the leading edge of migrating cells was carried out using ImagePro software and graphed as localization at the leading edge (% of cells) *versus* treatment ($n = 3 \pm$ S.D.). *, $p < 0.05$.

the triterpenoids. Rat2 fibroblasts were scratched and cells were then allowed to polarize to establish a leading edge before being treated with DMSO or 10 μM CK-869. The cells were then fixed, permeabilized, and stained for Arp3, n-WASp, and phalloidin. We observed that Arp3 and n-WASp co-localized at the leading edge of polarized cells in the absence of CK-869, however, both proteins were displaced from the leading edge and appeared diffused throughout the cytoplasm of the cell (Fig. 10). We also observed that phalloidin staining at the leading edge of polarized cells as well as actin staining were reduced in the CK-869-treated cells suggesting that the inhibition of branched actin polymerization alters cell polarity (Fig. 11). Taken together, our results suggest that synthetic triterpenoids target Arp2/3-dependent actin polymerization, which contributes to the inhibition of cell migration.

DISCUSSION

Cell migration plays an essential role in development, immune surveillance, and cellular repair. In cancer, it is the precursor event prior to most advanced cancer metastases. The diverse roles of cell migration make it difficult to understand its mechanisms of action clearly especially in the context of cancer, an illness that is made of multiple different diseases. Therefore, one of the major focuses in chemotherapy is to study the means of targeting cell migration to block tumor cells from migrating and invading other parts of the body. Here we show that synthetic triterpenoids, which are effective at inducing apoptosis and modulate reduction-oxidation reaction balance, are also effective at inhibiting cell migration. We observed that cell migration is inhibited by CDDO-Me and CDDO-Im in a dose-dependent manner, with 1 μM being most effective without inducing apoptosis over 16 h (Fig. 1). We also found that Arp3 was a novel triterpenoid-binding protein (Figs. 3 and 4). Arp3 is an important subunit of

the Arp2/3 complex, which is involved in the nucleation process of branched actin polymerization. Interestingly, the concentration of triterpenoids necessary to inhibit branched actin polymerization *in vitro* (50 μM) was higher than the concentration necessary to inhibit cell migration (1 μM). This may reflect the possibility that the relative ratios of purified proteins *in vitro* rendered the inhibiting compounds less active or that there are other triterpenoid targets in the cell that have yet to be identified. This second possibility is supported by our previous observation that the microtubule cytoskeleton is affected by CDDO-Im (49).

The knockdown of Arp2/3 using siRNA has been observed to reduce cell migration (Fig. 7). Our studies further show that the triterpenoids target Arp3 and inhibit cell migration by specifically affecting branched actin polymerization (Figs. 4–6). Branched actin polymerization is essential for the formation of the lamellipodia at the leading edge of migrating cells, which in turn allows for proper cell migration. Therefore, the reduction of branched actin polymerization by synthetic triterpenoids via Arp3 may provide a novel mechanism for which anti-cancer agents may be able to hinder cell migration and metastasis.

In this study, we also investigated whether the activities of small Rho GTPases would be affected by triterpenoid treatment. Although small Rho GTPases play a large role in cell migration, they do not seem to be major triterpenoid targets (supplemental Fig. S1). Interestingly, we found that Rac1 activity was slightly elevated by CDDO-Im, whereas the activities of the other Rho GTPases were not altered. This is contrary to what was expected with respect to the inhibition of cell migration. We reasoned that this could be due to a by-product of another triterpenoid-specific phenomenon that has yet to be determined.

Recently, Arp2/3 inhibitors have been characterized by Pollard and colleagues (52). These inhibitors bind to different sites of the Arp2/3 complex, thereby, inhibiting its nucleating function. Specifically, CK-636 binds between Arp2 and Arp3; consequently, preventing Arp2 and Arp3 from forming an active complex for nucleation. CK-548 and CK-869 associate with Arp3 at its hydrophobic core, resulting in a conformation change that blocks nucleation of branched actin. This novel insight on how the binding of Arp2/3 inhibitors modulates activation of the Arp2/3 complex may possibly be transferred to the synthetic triterpenoids. Indeed, we observed that CDDO-Me docked to Arp2/3 in the same hydrophobic pocket as CK-869 and was displaced in binding assays (Fig. 8). This was further corroborated with functional assays where *bona fide* Arp3 inhibition blocked cell migration and polarity (Figs. 9–11). We therefore conclude that CDDO-Im and CDDO-Me inhibit Arp2/3 function in a similar manner as the Arp3 inhibitors. Taken together, this suggests that a combined inhibition of microtubule and branched actin cytoskeletal dynamics are involved in triterpenoid-mediated reduction of cell migration.

Acknowledgments—We thank Dr. M. B. Sporn for the generous gift of the triterpenoids (CDDO-Im, CDDO-Me, b-CDDO-Me; Compound 6) used in this study. We also thank Boun Thai for excellent technical assistance.

REFERENCES

1. Ozdamar, B., Bose, R., Barrios-Rodiles, M., Wang, H. R., Zhang, Y., and Wrana, J. L. (2005) *Science* **307,** 1603–1609
2. Mehlen, P., and Puisieux, A. (2006) *Nat. Rev. Cancer* **6,** 449–458
3. Le Clainche, C., and Carlier, M. F. (2008) *Physiol. Rev.* **88,** 489–513
4. Ahmad, R., Raina, D., Meyer, C., Kharbanda, S., and Kufe, D. (2006) *J. Biol. Chem.* **281,** 35764–35769
5. Chintharlapalli, S., Papineni, S., Konopleva, M., Andreef, M., Samudio, I., and Safe, S. (2005) *Mol. Pharmacol.* **68,** 119–128
6. Deeb, D., Gao, X., Dulchavsky, S. A., and Gautam, S. C. (2007) *Anticancer Res.* **27,** 3035–3044
7. Gao, X., Deeb, D., Danyluk, A., Media, J., Liu, Y., Dulchavsky, S. A., and Gautam, S. C. (2008) *Immunopharmacol. Immunotoxicol.* **30,** 581–600
8. Liby, K., Voong, N., Williams, C. R., Risingsong, R., Royce, D. B., Honda, T., Gribble, G. W., Sporn, M. B., and Letterio, J. J. (2006) *Clin. Cancer Res.* **12,** 4288–4293
9. Liby, K. T., Yore, M. M., and Sporn, M. B. (2007) *Nat. Rev. Cancer* **7,** 357–369
10. Ling, X., Konopleva, M., Zeng, Z., Ruvolo, V., Stephens, L. C., Schober, W., McQueen, T., Dietrich, M., Madden, T. L., and Andreeff, M. (2007) *Cancer Res.* **67,** 4210–4218
11. Shin, S., Wakabayashi, N., Misra, V., Biswal, S., Lee, G. H., Agoston, E. S., Yamamoto, M., and Kensler, T. W. (2007) *Mol. Cell. Biol.* **27,** 7188–7197
12. Shishodia, S., Sethi, G., Konopleva, M., Andreeff, M., and Aggarwal, B. B. (2006) *Clin. Cancer Res.* **12,** 1828–1838
13. Thimmulappa, R. K., Fuchs, R. J., Malhotra, D., Scollick, C., Traore, K., Bream, J. H., Trush, M. A., Liby, K. T., Sporn, M. B., Kensler, T. W., and Biswal, S. (2007) *Antioxid. Redox Signal.* **9,** 1963–1970
14. Thimmulappa, R. K., Scollick, C., Traore, K., Yates, M., Trush, M. A., Liby, K. T., Sporn, M. B., Yamamoto, M., Kensler, T. W., and Biswal, S. (2006) *Biochem. Biophys. Res. Commun.* **351,** 883–889
15. Wang, Y., Porter, W. W., Suh, N., Honda, T., Gribble, G. W., Leesnitzer, L. M., Plunket, K. D., Mangelsdorf, D. J., Blanchard, S. G., Willson, T. M., and Sporn, M. B. (2000) *Mol. Endocrinol.* **14,** 1550–1556
16. Yates, M. S., Kwak, M. K., Egner, P. A., Groopman, J. D., Bodreddigari, S., Sutter, T. R., Baumgartner, K. J., Roebuck, B. D., Liby, K. T., Yore, M. M., Honda, T., Gribble, G. W., Sporn, M. B., and Kensler, T. W. (2006) *Cancer Res.* **66,** 2488–2494
17. Yates, M. S., Tauchi, M., Katsuoka, F., Flanders, K. C., Liby, K. T., Honda, T., Gribble, G. W., Johnson, D. A., Johnson, J. A., Burton, N. C., Guilarte, T. R., Yamamoto, M., Sporn, M. B., and Kensler, T. W. (2007) *Mol. Cancer Ther.* **6,** 154–162
18. Yore, M. M., Liby, K. T., Honda, T., Gribble, G. W., and Sporn, M. B. (2006) *Mol. Cancer Ther.* **5,** 3232–3239
19. Honda, T., Honda, Y., Favaloro, F. G., Jr., Gribble, G. W., Suh, N., Place, A. E., Rendi, M. H., and Sporn, M. B. (2002) *Bioorg. Med. Chem. Lett.* **12,** 1027–1030
20. Honda, T., Rounds, B. V., Bore, L., Favaloro, F. G., Jr., Gribble, G. W., Suh, N., Wang, Y., and Spor, M. B. (1999) *Bioorg. Med. Chem. Lett.* **9,** 3429–3434
21. Honda, T., Rounds, B. V., Bore, L., Finlay, H. J., Favaloro, F. G., Jr., Suh, N., Wang, Y., Sporn, M. B., and Gribble, G. W. (2000) *J. Med. Chem.* **43,** 4233–4246
22. Honda, T., Rounds, B. V., Gribble, G. W., Suh, N., Wang, Y., and Sporn, M. B. (1998) *Bioorg. Med. Chem. Lett.* **8,** 2711–2714
23. Ikeda, T., Nakata, Y., Kimura, F., Sato, K., Anderson, K., Motoyoshi, K., Sporn, M., and Kufe, D. (2004) *Mol. Cancer Ther.* **3,** 39–45
24. Ikeda, T., Sporn, M., Honda, T., Gribble, G. W., and Kufe, D. (2003) *Cancer Res.* **63,** 5551–5558
25. Suh, N., Wang, Y., Honda, T., Gribble, G. W., Dmitrovsky, E., Hickey, W. F., Maue, R. A., Place, A. E., Porter, D. M., Spinella, M. J., Williams, C. R., Wu, G., Dannenberg, A. J., Flanders, K. C., Letterio, J. J., Mangelsdorf, D. J., Nathan, C. F., Nguyen, L., Porter, W. W., Ren, R. F., Roberts, A. B., Roche, N. S., Subbaramaiah, K., and Sporn, M. B. (1999) *Cancer Res.* **59,** 336–341
26. Kress, C. L., Konopleva, M., Martínez-García, V., Krajewska, M., Lefebvre, S., Hyer, M. L., McQueen, T., Andreeff, M., Reed, J. C., and Zapata, J. M.

(2007) *PLoS ONE* **2,** e559
27. Brookes, P. S., Morse, K., Ray, D., Tompkins, A., Young, S. M., Hilchey, S., Salim, S., Konopleva, M., Andreeff, M., Phipps, R., and Bernstein, S. H. (2007) *Cancer Res.* **67,** 1793–1802
28. Han, S. S., Peng, L., Chung, S. T., DuBois, W., Maeng, S. H., Shaffer, A. L., Sporn, M. B., and Janz, S. (2006) *Mol. Cancer* **5,** 22
29. Inoue, S., Snowden, R. T., Dyer, M. J., and Cohen, G. M. (2004) *Leukemia* **18,** 948–952
30. Ray, D. M., Morse, K. M., Hilchey, S. P., Garcia, T. M., Felgar, R. E., Maggirwar, S. B., Phipps, R. P., and Bernstein, S. H. (2006) *Exp. Hematol.* **34,** 1202–1211
31. Ito, Y., Pandey, P., Place, A., Sporn, M. B., Gribble, G. W., Honda, T., Kharbanda, S., and Kufe, D. (2000) *Cell Growth & Differ.* **11,** 261–267
32. Konopleva, M., Contractor, R., Kurinna, S. M., Chen, W., Andreeff, M., and Ruvolo, P. P. (2005) *Leukemia* **19,** 1350–1354
33. Konopleva, M., Tsao, T., Estrov, Z., Lee, R. M., Wang, R. Y., Jackson, C. E., McQueen, T., Monaco, G., Munsell, M., Belmont, J., Kantarjian, H., Sporn, M. B., and Andreeff, M. (2004) *Cancer Res.* **64,** 7927–7935
34. Konopleva, M., Tsao, T., Ruvolo, P., Stiouf, I., Estrov, Z., Leysath, C. E., Zhao, S., Harris, D., Chang, S., Jackson, C. E., Munsell, M., Suh, N., Gribble, G., Honda, T., May, W. S., Sporn, M. B., and Andreeff, M. (2002) *Blood* **99,** 326–335
35. Stadheim, T. A., Suh, N., Ganju, N., Sporn, M. B., and Eastman, A. (2002) *J. Biol. Chem.* **277,** 16448–16455
36. Gao, X., Deeb, D., Jiang, H., Liu, Y., Dulchavsky, S. A., and Gautam, S. C. (2007) *J. Neurooncol.* **84,** 147–157
37. Ito, Y., Pandey, P., Sporn, M. B., Datta, R., Kharbanda, S., and Kufe, D. (2001) *Mol. Pharmacol.* **59,** 1094–1099
38. Kim, K. B., Lotan, R., Yue, P., Sporn, M. B., Suh, N., Gribble, G. W., Honda, T., Wu, G. S., Hong, W. K., and Sun, S. Y. (2002) *Mol. Cancer Ther.* **1,** 177–184
39. Liby, K., Royce, D. B., Williams, C. R., Risingsong, R., Yore, M. M., Honda, T., Gribble, G. W., Dmitrovsky, E., Sporn, T. A., and Sporn, M. B. (2007) *Cancer Res.* **67,** 2414–2419
40. Zou, W., Chen, S., Liu, X., Yue, P., Sporn, M. B., Khuri, F. R., and Sun, S. Y. (2007) *Cancer Biol. Ther.* **6,** 1614–1620
41. Zou, W., Liu, X., Yue, P., Zhou, Z., Sporn, M. B., Lotan, R., Khuri, F. R., and Sun, S. Y. (2004) *Cancer Res.* **64,** 7570–7578
42. Lapillonne, H., Konopleva, M., Tsao, T., Gold, D., McQueen, T., Sutherland, R. L., Madden, T., and Andreeff, M. (2003) *Cancer Res.* **63,** 5926–5939
43. Hyer, M. L., Croxton, R., Krajewska, M., Krajewski, S., Kress, C. L., Lu, M., Suh, N., Sporn, M. B., Cryns, V. L., Zapata, J. M., and Reed, J. C. (2005) *Cancer Res.* **65,** 4799–4808
44. Konopleva, M., Zhang, W., Shi, Y. X., McQueen, T., Tsao, T., Abdelrahim, M., Munsell, M. F., Johansen, M., Yu, D., Madden, T., Safe, S. H., Hung, M. C., and Andreeff, M. (2006) *Mol. Cancer Ther.* **5,** 317–328
45. Melichar, B., Konopleva, M., Hu, W., Melicharova, K., Andreeff, M., and Freedman, R. S. (2004) *Gynecol. Oncol.* **93,** 149–154
46. Samudio, I., Konopleva, M., Hail, N., Jr., Shi, Y. X., McQueen, T., Hsu, T., Evans, R., Honda, T., Gribble, G. W., Sporn, M., Gilbert, H. F., Safe, S., and Andreeff, M. (2005) *J. Biol. Chem.* **280,** 36273–36282
47. Pedersen, I. M., Kitada, S., Schimmer, A., Kim, Y., Zapata, J. M., Charboneau, L., Rassenti, L., Andreeff, M., Bennett, F., Sporn, M. B., Liotta, L. D., Kipps, T. J., and Reed, J. C. (2002) *Blood* **100,** 2965–2972
48. Suh, W. S., Kim, Y. S., Schimmer, A. D., Kitada, S., Minden, M., Andreeff, M., Suh, N., Sporn, M., and Reed, J. C. (2003) *Leukemia* **17,** 2122–2129
49. To, C., Kulkarni, S., Pawson, T., Honda, T., Gribble, G. W., Sporn, M. B., Wrana, J. L., and Di Guglielmo, G. M. (2008) *J. Biol. Chem.* **283,** 11700–11713
50. Honda, T., Janosik, T., Honda, Y., Han, J., Liby, K. T., Williams, C. R., Couch, R. D., Anderson, A. C., Sporn, M. B., and Gribble, G. W. (2004) *J. Med. Chem.* **47,** 4923–4932
51. Morris, G. M., Huey, R., Lindstrom, W., Sanner, M. F., Belew, R. K., Goodsell, D. S., and Olson, A. J. (2009) *J. Comput. Chem.* **30,** 2785–2791
52. Nolen, B. J., Tomasevic, N., Russell, A., Pierce, D. W., Jia, Z., McCormick, C. D., Hartman, J., Sakowicz, R., and Pollard, T. D. (2009) *Nature* **460,** 1031–1034
53. Bore, L., Honda, T., Gribble, G. W., Lork, E., and Jasinski, J. P. (2002) *Acta Crystallogr. Sect. C Cryst. Struct. Chem.* **58,** 199–200
54. Sogno, I., Vannini, N., Lorusso, G., Cammarota, R., Noonan, D. M., Generoso, L., Sporn, M. B., and Albini, A. (2009) *Recent Res. Cancer Res.* **181,** 209–212
55. Couch, R. D., Ganem, N. J., Zhou, M., Popov, V. M., Honda, T., Veenstra, T. D., Sporn, M. B., and Anderson, A. C. (2006) *Mol. Pharmacol.* **69,** 1158–1165
56. Fukata, M., Nakagawa, M., and Kaibuchi, K. (2003) *Curr. Opin. Cell Biol.* **15,** 590–597